Towards Superresolution Surface Metrology: Quantum Estimation of Angular and Axial Separations. — Source link

Carmine Napoli, Samanta Piano, Richard Leach, Gerardo Adesso ...+1 more authors

Institutions: University of Nottingham

Related papers:

- Quantum Limited Superresolution of an Incoherent Source Pair in Three Dimensions.

- Quantum Theory of Superresolution for Two Incoherent Optical Point Sources

- Multiparameter quantum metrology of incoherent point sources: Towards realistic superresolution

- Achieving the ultimate optical resolution

- Statistical distance and the geometry of quantum states

Towards Superresolution Surface Metrology: Quantum Estimation of Angular and Axial Separations

Carmine Napoli,[1,2,*] Samanta Piano,[2,†] Richard Leach,[2,‡] Gerardo Adesso,[1,§] and Tommaso Tufarelli[1,‖]

[1]*School of Mathematical Sciences and Centre for the Mathematics and Theoretical Physics of Quantum Non-Equilibrium Systems, University of Nottingham, University Park Campus, Nottingham NG7 2RD, United Kingdom*
[2]*Manufacturing Metrology Team, Faculty of Engineering, University of Nottingham, Jubilee Campus, Nottingham NG8 1BB, United Kingdom*

We investigate the localization of two incoherent point sources with arbitrary angular and axial separations in the paraxial approximation. By using quantum metrology techniques, we show that a simultaneous estimation of the two separations is achievable by a single quantum measurement, with a precision saturating the ultimate limit stemming from the quantum Cramér-Rao bound. Such a precision is not degraded in the subwavelength regime, thus overcoming the traditional limitations of classical direct imaging derived from Rayleigh's criterion. Our results are qualitatively independent of the point spread function of the imaging system, and quantitatively illustrated in detail for the Gaussian instance. This analysis may have relevant applications in three-dimensional surface measurements.

Introduction.—High-resolution imaging is a cornerstone of modern science and engineering, which has enabled revolutionary advances in astronomy, manufacturing, biochemistry, and medical diagnostics. In traditional direct imaging based on classical wave optics, two incoherent point sources with angular separation smaller than the wavelength of the emitted light cannot be resolved due to fundamental diffraction effects [1], a phenomenon recently dubbed "Rayleigh's curse" [2]. Several techniques, including most prominently fluorescence microscopy [3], have been introduced in recent years to overcome this limitation and achieve sub-wavelength imaging [4,5]. Nevertheless, to determine the ultimate limits of optical resolution one needs to resort to a full quantum mechanical description of the imaging process [6]. In this respect, a breakthrough has been reported in a series of works [2,7–18] initiated by Tsang and collaborators [2], who employed techniques from quantum metrology [19–22] to prove that the achievable error in estimating the angular separation of two incoherent point sources, in the paraxial approximation, is in fact independent of said separation (no matter how small), provided an optimal detection scheme is performed on the image plane. These results, which stem from the fundamental quantum Cramér-Rao bound [19,20] and *de facto* banish Rayleigh's curse [2], have been corroborated by proof-of-principle experiments [23–26].

The majority of the studies presented so far on quantum superlocalization, however, were limited to the case of point sources aligned on the same object plane, thus neglecting their axial separation. The optical lateral resolution of an imaging system is an important characteristic, but it is not the only figure of merit relevant for the measurement of nonflat surfaces [27]. When probing surface topography, the spacing of the points in an image must be considered, along with the ability to accurately determine the heights of features. In other words, the lateral resolution must be considered in conjunction with the ability of the system to transfer surface amplitudes [28].

To address this key issue, in this Letter we consider the simultaneous estimation of both angular and axial separations, as well as the corresponding centroid coordinates, of two incoherent point sources aligned in general on different object planes. These point sources may model, e.g., two emitters at the edges of a steep section on a rough surface, as indicated by the red dotted outline in Fig. 1.

We tackle the problem by resorting to the toolbox of multiparameter quantum metrology, a branch of quantum technology that is attracting increasing interest thanks to its prominent role in fundamental science and applications [19–22,29–51]. We find that Rayleigh's curse does not occur even when the sources have a nonzero axial separation, and both axial and angular distances can be
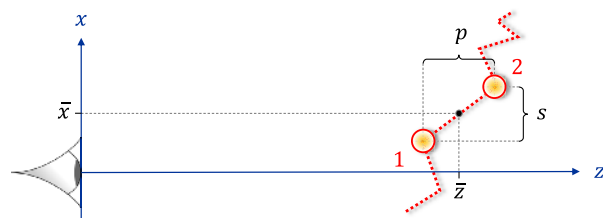

FIG. 1. Schematic of the two sources. The four parameters to be estimated are the angular separation s, the axial separation p, the angular centroid coordinate $\bar{x}$, and the axial centroid coordinate $\bar{z}$.

estimated simultaneously and with distance-independent precision by means of a single optimal quantum measurement, meeting the compatibility requirements for saturation of the multiparameter quantum Cramér-Rao bound [29,32]. These results are obtained analytically and are valid for any point spread function of the imaging system obeying the paraxial wave equation. We then specialize to the illustrative case of a Gaussian point spread function, and derive closed formulas for the achievable estimation error and its scaling with the parameters of interest as determined by the quantum Fisher information matrix, showing that in the limit of small angular and axial distances all the parameters, including the centroid coordinates, become statistically independent.

Sources and imaging system model.—We address the problem of estimating both axial and angular separation of two point sources by following a similar approach to Ref. [2], which is in turn inspired by Rayleigh's work [1]. We assume that the detectable light on the image plane can be described as an incoherent mixture of two quasimonochromatic scalar paraxial waves, one coming from each source. As shown in Fig. 1, our two sources are in general not lying on the same object plane (an "object plane" is a plane perpendicular to the optical axis z), and they feature an angular separation s and an axial separation p.

Considering thermal sources at optical frequencies, we divide the total emission time into short coherence time intervals τ_c, so that within each interval the sources can be assumed weak, i.e., effectively emitting at most one photon. This is a standard approach for modeling incoherent thermal sources [52–58], and it allows us to describe the quantum state ρ of the optical field on the image plane as a mixture of a zero-photon state ρ_0 and a one-photon state ρ_1 in each time interval (neglecting contributions from higher photon numbers) [59],

$$\rho = (1 - \varepsilon)\rho_0 + \varepsilon\rho_1 + o(\varepsilon^2), \qquad (1)$$

where $\varepsilon \ll 1$ is the average number of photons impinging on the image plane. In practice, a detectable signal is obtained by measuring the optical field for a time $t \gg \tau_c$, so that many coherence time intervals are included, resulting in a non-negligible mean photon number.

We assume in general that the image-plane field amplitude generated by each source takes the form

$$\Psi_j(x, y) \equiv \psi(x - x_j, y, z_j), \qquad (2)$$

where (x, y) are the image-plane coordinates, (x_j, z_j) are the unknown coordinates of the sources $j = 1, 2$, x_j being the coordinate perpendicular to the optical axis, and z_j the axial distance to the image plane (in this Letter we assume that the other coordinate $y_j = 0$ is known). The amplitude function $\psi(x, y, z)$ obeys a paraxial wave equation of the form

$$i\partial_z\psi = G\psi, \qquad (3)$$

where G is a self-adjoint differential operator featuring only x and y derivatives—for example, in free space one would have $G = \frac{1}{2k}(\partial_x^2 + \partial_y^2) + k$, k being the wave number. Since $[G, \partial_x] = 0$, it follows that $\Psi_j(x, y) = \exp(-iGz_j - x_j\partial_x)\psi(x, y, 0)$.

We shall indicate with $a(x, y)$ the field annihilation operator at position (x, y) on the image plane, satisfying the bosonic commutation rule $[a(x, y), a^\dagger(x', y')] = \delta(x - x')\delta(y - y')$.

We can then write the state ρ_1 as the incoherent mixture

$$\rho_1 = \frac{1}{2}(|\Psi_1\rangle\langle\Psi_1| + |\Psi_2\rangle\langle\Psi_2|), \qquad (4)$$

where the quantum state of the optical field on the image plane corresponding to the emission of one photon by the source r may be expressed as

$$|\Psi_j\rangle = \exp(-iGz_j - x_j\partial_x)|\psi\rangle, \qquad (5)$$

$$|\psi\rangle \equiv \int_{\mathbb{R}^2} \psi(x, y, 0)a^\dagger(x, y)|0\rangle\,dxdy, \qquad (6)$$

with $|0\rangle$ being the field vacuum state. Finally, we may take $\psi(x, y, 0)$ real, which results in some simplifications later on. This can be assumed without loss of generality, as the complex phase of $\psi(x, y, 0)$ may be compensated by a redefinition of $a(x, y)$ that is independent of the source parameters. However, $\psi(x, y, z)$ will have in general a nontrivial phase profile.

Multiparameter estimation and quantum Cramér-Rao bound.—We work under the assumption that the photon statistics of our sources is Poissonian, following a similar approach as in Ref. [2]. We can thus assume that in a single run of the experiment, which lasts for M coherence time intervals, M copies of the state ρ in Eq. (1) are prepared and measured (equivalently, one may consider the input state $\rho^{\otimes M}$). On average, this yields $M\varepsilon$ photons per run. In order to apply the standard tools of estimation theory, we further assume that $\nu \gg 1$ runs are performed, after which the measurement data are processed to build estimators for the unknown parameters.

In our case, the parameters of interest are the angular and axial relative coordinates and the centroid coordinates of the sources, indicated as $s, \bar{x}, p, \bar{z}$, see Fig. 1. We thus write the state ρ as a function of four parameters $\{\lambda_\mu\}_{\mu=1,\ldots,4}$, where

$$\lambda_1 \equiv s = x_2 - x_1, \qquad \lambda_2 \equiv \bar{x} = \frac{x_2 + x_1}{2},$$

$$\lambda_3 \equiv p = z_2 - z_1, \qquad \lambda_4 \equiv \bar{z} = \frac{z_2 + z_1}{2}. \qquad (7)$$

The statistical error (variance) $\Delta\lambda_\mu^2$ of any *unbiased* estimator of the unknown parameter λ_μ is lower bounded via the quantum Cramér-Rao bound (qCRb) [19,20]

$$\sum_{\mu=1}^{4} \Delta\lambda_\mu^2 \geq \frac{1}{\nu M\varepsilon} \mathrm{Tr}[H^{-1}], \qquad (8)$$

where H is the quantum Fisher information matrix (qFim) of the single-photon state ρ_1 (equivalently, this can be seen as the qFim per coherence time interval per photon). The prefactor on the right-hand side of Eq. (8) is obtained by exploiting the additivity property $\mathrm{qFim}(\rho^{\otimes M}) = M \times \mathrm{qFim}(\rho)$, and by approximating that $\mathrm{qFim}(\rho) \simeq \varepsilon \times \mathrm{qFim}(\rho_1)$ at leading order in ε (since the field vacuum state ρ_0 is independent of all source parameters and is always orthogonal to ρ_1—see also the discussion in the Appendix of Ref. [2]). The resulting linear dependence on the total photon number $\nu M\varepsilon$ is characteristic of classical light sources [22,60].

The qCRb suggests that, the higher the qFIm element $H_{\mu\mu}$, the more precisely (i.e., with lower statistical error) one may be able to estimate the parameter λ_μ, by performing a suitable measurement. While for a single parameter the qCRb can always be saturated asymptotically by means of an adaptive procedure [21], this is no longer the case for multiparameter estimation, as the parameters may not always be compatible [32]; we will discuss this issue in detail later in the Letter.

Results.—We recall that the qFim elements are given by

$$H_{\mu\nu} = \mathrm{Re}[\mathrm{Tr}(\rho_1 L_\mu L_\nu)], \qquad (9)$$

where L_μ is the symmetric logarithmic derivative (SLD) for the parameter λ_μ, defined implicitly by the equation

$$2\frac{\partial\rho_1}{\partial\lambda_\mu} = L_\mu\rho_1 + \rho_1 L_\mu. \qquad (10)$$

The following matrix (proportional to the averaged SLD commutators) will also be of interest for our discussion,

$$\Gamma_{\mu\nu} \equiv \mathrm{Im}[\mathrm{Tr}(\rho_1 L_\mu L_\nu)]. \qquad (11)$$

For the problem under investigation, we have derived general analytical expressions for both matrices H and Γ, as presented in detail in Appendix A [61]. Our derivation relies on the expansion of ρ_1 in the generally *nonorthogonal* basis

$$\{|\Psi_1\rangle, |\Psi_2\rangle, \partial_{x_1}|\Psi_1\rangle, \partial_{z_1}|\Psi_1\rangle, \partial_{x_2}|\Psi_2\rangle, \partial_{z_2}|\Psi_2\rangle\}, \quad (12)$$

followed by standard linear algebraic manipulations. This method results in significant simplifications over previous studies of quantum superlocalization (typically relying on

the explicit construction of an orthogonal basis to span the support of ρ_1 and its derivatives, as, e.g., in Ref. [2]), and may be of independent interest in its own right for the field of multiparameter quantum metrology. Thanks to the representation of $|\Psi_j\rangle$ given in Eq. (5), it is easy to check that all the scalar products between the above basis vectors only depend on $s = x_2 - x_1$ and $p = z_2 - z_1$, which in turn implies that the qFim is independent of the centroid coordinates $\bar{x}$ and $\bar{z}$. The corresponding physical interpretation is that the information content of the emitted light is not affected by propagation along the optical axis, or by a redefinition of the image plane origin. Additional simplifications follow from our assumption $\psi(x, y, 0) \in \mathbb{R}$, which implies $\langle\psi|\partial_x\psi\rangle = 0$. We then find that the qFim is composed of the diagonal elements

$$H_{ss} = \langle\partial_x\psi|\partial_x\psi\rangle, \qquad H_{pp} = \Delta G^2, \qquad (13)$$

$$H_{\bar{x}\bar{x}} = 4\langle\partial_x\psi|\partial_x\psi\rangle - 4(\partial_s|\gamma|)^2 - 4\frac{|\gamma|^2(\partial_s\varphi)^2}{1-|\gamma|^2}, \qquad (14)$$

$$H_{\bar{z}\bar{z}} = \frac{4}{1-|\gamma|^2}\{\Delta G^2 - (\partial_p|\gamma|)^2 - |\gamma|^2[\langle G^2\rangle - (\partial_p|\gamma|)^2 + 2\langle G\rangle\partial_p\varphi + (\partial_p\varphi)^2]\}, \qquad (15)$$

while the off-diagonal elements are all zero except

$$H_{\bar{x}\bar{z}} = -\frac{4|\gamma|^2(\partial_s\varphi)(\langle G\rangle + \partial_p\varphi)}{1-|\gamma|^2} - 4(\partial_s|\gamma|)(\partial_p|\gamma|). \quad (16)$$

At the same time, the only nonzero matrix elements of Γ are

$$\Gamma_{s\bar{x}} = -\frac{2|\gamma|^3(\partial_s|\gamma|)(\partial_s\varphi)}{1-|\gamma|^2}, \qquad (17)$$

$$\Gamma_{p\bar{z}} = -\frac{2|\gamma|^3(\partial_p|\gamma|)(\langle G\rangle + \partial_p\varphi)}{1-|\gamma|^2}, \qquad (18)$$

$$\Gamma_{s\bar{z}} = 2|\gamma|\left((\partial_p|\gamma|)(\partial_s\varphi) - \frac{\partial_s|\gamma|(\partial_s\varphi + \langle G\rangle)}{1-|\gamma|^2}\right), \qquad (19)$$

$$\Gamma_{\bar{x}p} = 2|\gamma|\left(-(\partial_s|\gamma|)(\langle G\rangle + \partial_p\varphi) + \frac{(\partial_p|\gamma|)(\partial_s\varphi)}{1-|\gamma|^2}\right). \qquad (20)$$

The following short-hand notations have been used:

$$\gamma \equiv \langle\Psi_1|\Psi_2\rangle, \qquad \varphi \equiv \arg\gamma, \qquad (21)$$

$$\langle O\rangle \equiv \langle\psi|O|\psi\rangle, \qquad \Delta G^2 \equiv \langle G^2\rangle - \langle G\rangle^2, \qquad (22)$$

where we emphasize that $\gamma = \gamma(s, p)$ is the only quantity depending on the source coordinates. A fundamental result can be immediately inferred from Eq. (13) and below: for any point spread function that satisfies the paraxial wave

equation, H_{ss} and H_{pp} are *constant*. This statement exemplifies how our results provide new insights on the problem of subwavelength imaging, while correctly reproducing what is known for $p = 0$ [2]. We note in particular that Rayleigh's curse does not affect the estimation of the angular separation s nor that of the axial separation p.

Taking one step further, we can now investigate how close one can get to the limits imposed by the qCRb in practical experiments. In quantum estimation theory, multi-parameter problems embody a nontrivial generalization of the single-parameter case [21,29,31,32]: if an estimation scheme is optimized for a particular parameter, it typically results into an increased error in estimating the others. However, in the best case scenario, such a trade-off does not apply, and one can identify an optimal protocol for the estimation of all the parameters simultaneously. This happens if and only if the parameters are *compatible*; i.e., they satisfy the following conditions [32]: (i) There is a single probe state yielding the maximal qFim element for each of the parameters; (ii) there is a single measurement which is jointly optimal for extracting information on all the parameters from the output state, ensuring the asymptotic saturability of the qCRb; (iii) the parameters are statistically independent, meaning that the indeterminacy of one of them does not affect the error on estimating the others. We recall also that (ii) holds if and only if $\Gamma_{\mu\nu} = 0 \ \forall \ \mu \neq \nu$, while (iii) is equivalent to the condition $H_{\mu\nu} = 0 \ \forall \ \mu \neq \nu$.

In this Letter we do not focus on the first condition, since our theory is built around a realistic imaging scenario in which the emission properties of the sources are fixed in advance. Yet, it is worth investigating conditions (ii) and (iii), since they have crucial implications for the actual achievability of the statistical errors given by the qCRb. Remarkably, we find that conditions (ii) and (iii) are always satisfied for the pair of parameters (s, p)—independently of the specifics of the point spread function. In the simplified scenario where $(\bar{x}, \bar{z})$ are estimated independently or known in advance, it is thus possible to construct a physical measurement and estimation strategy for s and p saturating Eq. (8) asymptotically [29,32]. On the other hand, we can see that conditions (ii) and (iii) do not hold in general for the full set of parameters $(s, p, \bar{x}, \bar{z})$. Yet, we shall see in the example below that there is at least one relevant type of point spread function for which conditions (ii) and (iii) are satisfied for all parameters in the limit $s \to 0, p \to 0$.

We consider in what follows a Gaussian beam in free space,

$$\psi(x, y, z) = \sqrt{\frac{kz_R}{\pi}} \frac{i}{z + iz_R} \exp\left(\frac{-ik(x^2 + y^2)}{2(z + iz_R)} - ikz\right),$$

(23)

where z_R is a length parameter characterizing the beam, typically assumed of the same order as the wavelength, i.e., $\sim 1/k$. Equation (23) can be obtained, e.g., if the fields generated by the two sources are well approximated by Gaussian beams in the vicinity of the image plane [62]. We thus obtain

$$\gamma = \frac{2iz_R}{p + 2iz_R} \exp\left(-ikp - \frac{i}{2}\frac{ks^2}{p + 2iz_R}\right),$$

$$\langle \partial_x \psi | \partial_x \psi \rangle = \frac{k}{2z_R},$$

$$\langle G \rangle = k - \frac{1}{2z_R},$$

$$\langle G^2 \rangle = k^2 - \frac{k}{z_R} + \frac{1}{2z_R^2}.$$

(24)

By substituting the above expressions in the qFim elements calculated previously, we find fully analytical closed formulas (as reported in Appendix B [61]) that allow us to perform a comprehensive analysis of the multiparameter estimation problem under investigation. Furthermore, the Gaussian case bears the advantage that it can be easily compared with the existing literature that tackled the estimation of s alone (typically fixing $p = 0$). To support the solidity of our results, we have indeed checked that, in the limit $p \to 0$, our expressions for H_{ss} and $H_{\bar{x}\bar{x}}$ match the appropriate quantities in Refs. [2,60].

Our results become particularly interesting in the regime $ks, kp \ll 1$, which is precisely the one of relevance to subwavelength imaging. In this limit we have

$$\lim_{(s,p)\to(0,0)} H = \text{diag}\left\{\frac{k}{2z_R}, \frac{2k}{z_R}, \frac{1}{4z_R^2}, \frac{1}{z_R^2}\right\},$$

(25)

$$\lim_{(s,p)\to(0,0)} \Gamma = \text{diag}\{0, 0, 0, 0\},$$

(26)

meaning that the (optimal) estimators of the four parameters $s, \bar{x}, p, \bar{z}$ are approximately statistically independent; i.e., they have vanishingly small statistical correlations, when the two sources have infinitesimal angular and axial separations.

The behavior of the four diagonal qFim elements $H_{\mu\mu}$ as a function of the separations s and p is illustrated in Fig. 2; the top panel can be compared directly with Fig. 2 of Ref. [2]. From the plots and from Eq. (25), we see that the qFIm diagonal elements tend to a nonzero value when $s, p \to 0$. Hence the fundamental lower bound on the total estimation error, $\propto \text{Tr}[H^{-1}]$, stays finite even when the two sources are infinitesimally close, instead of diverging as in direct imaging [1,2]. Equation (26) further suggests that it should be possible to construct a single measurement that is approximately optimal for the estimation of *all four parameters* when $ks, kp \ll 1$. Note that this may require
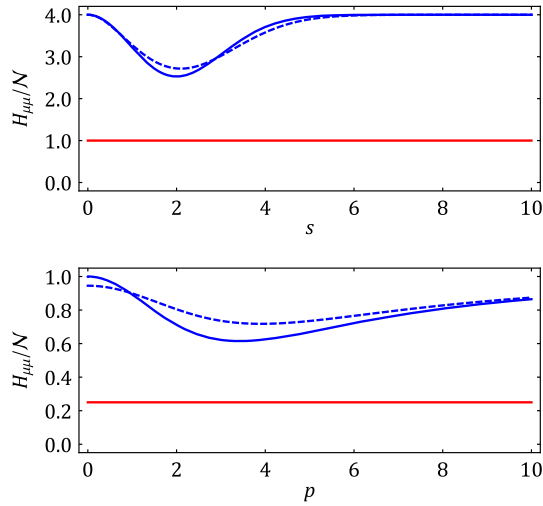
FIG. 2. Top: Angular localization. Plots of the qFim elements H_{ss} (red, lowermost curve) and $H_{\bar{x}\bar{x}}$ (blue, uppermost curves), versus the angular separation s; continuous lines refer to $p = 0$ and dashed lines to $p = 2$. Bottom: Axial localization. Plots of the qFim elements H_{pp} (red, lowermost curve) and $H_{\bar{z}\bar{z}}$ (blue, uppermost curves), versus the axial separation p; continuous lines are for $s = 0$ and dashed lines for $s = 1$. The results are for Gaussian beams with $k = 1, z_R = 2$. The vertical axes are normalized to $\mathcal{N} = \frac{1}{2} k / z_R$.

collective measurements over many copies, i.e., many time intervals. Exploring more practical suboptimal strategies and determining how close one can get to the optimal measurement by using only single-copy measurements will be the subject of future work.

Conclusions.—We determined the ultimate quantum limits to the simultaneous estimation of both angular and axial separations and centroid coordinates of two incoherent point sources on different object planes in the paraxial approximation. Our results indicate that there exists a jointly optimal detection scheme that enables resolving the sources even when arbitrarily close, reasserting that Rayleigh's curse is merely an artifact of classical detection strategies based on direct imaging. In practice, a measurement apparatus approaching the optimal precision can be designed by adapting the methods of Refs. [15,16,46,47,63], in particular extending the "spatial-mode demultiplexing" or "superlocalization by image inversion interferometry" techniques [2,7] to the axially separated setting considered here.

While some of our findings were illustrated explicitly for Gaussian beams, our framework is general and can be applied to any point spread function that satisfies the paraxial wave equation, thanks to the exact expressions in Eqs. (13)–(20). This leads to qualitatively similar results as those presented here. In particular, the two most important conclusions, namely, that the qFim elements for the angular distance s and for the axial distance p are both independent of s and p, and that the joint estimation of s and p fulfils the measurement compatibility condition

leading to the saturation of the quantum Cramér-Rao bound in Eq. (8), are in fact valid for any point spread function.

This Letter constitutes an important application of multiparameter quantum estimation theory to a realistic imaging setting, extending the seminal work of Ref. [2]. Our analysis, combined with the one in Ref. [12], yields a quantum enhanced toolbox for full 3D subwavelength localization. This paves the way to further experimental demonstrations and innovative metrology solutions in scientific, industrial, and biomedical domains, such as subnanometer depth mapping in rough surfaces, and dynamical interaction analysis of heterogeneous molecules in a cellular environment [4,5,27,64].

Note added.—Shortly after the initial submission of this Letter, quantum superresolution of two incoherent point sources in three dimensions was studied independently in Ref. [65], reporting explicit results for the case of a clear circular aperture.

[*]carmine.napoli@nottingham.ac.uk
[†]samanta.piano@nottingham.ac.uk
[‡]richard.leach@nottingham.ac.uk
[§]gerardo.adesso@nottingham.ac.uk
[‖]tommaso.tufarelli@nottingham.ac.uk

[1] L. Rayleigh, Xxxi. Investigations in optics, with special reference to the spectroscope, London Edinburgh Dublin Philos. Mag. J. Sci. **8**, 261 (1879).

[2] M. Tsang, R. Nair, and X.-M. Lu, Quantum Theory of Superresolution for Two Incoherent Optical Point Sources, Phys. Rev. X **6**, 031033 (2016).

[3] L. Möckl, D. C. Lamb, and C. Bruchle, Super-resolved fluorescence microscopy: Nobel Prize in chemistry 2014 for Eric Betzig, Stefan Hell, and William E. Moerner, Angew. Chem., Int. Ed. Engl. **53**, 13972 (2014).

[4] W. E. Moerner, New directions in single-molecule imaging and analysis, Proc. Natl. Acad. Sci. U.S.A. **104**, 12596 (2007).

[5] R. Leach and B. Sherlock, Applications of super-resolution imaging in the field of surface topography measurement, Surf. Topogr.: Metrol. Prop. **2**, 023001 (2014).

[6] M. Genovese, Real applications of quantum imaging, J. Opt. 18, 073002 (2016).

[7] R. Nair and M. Tsang, Interferometric superlocalization of two incoherent optical point sources, Opt. Express 24, 3684 (2016).

[8] R. Nair and M. Tsang, Far-Field Superresolution of Thermal Electromagnetic Sources at the Quantum Limit, Phys. Rev. Lett. 117, 190801 (2016).

[9] C. Lupo and S. Pirandola, Ultimate Precision Bound of Quantum and Subwavelength Imaging, Phys. Rev. Lett. 117, 190802 (2016).

[10] M. Tsang, Subdiffraction incoherent optical imaging via spatial-mode demultiplexing, New J. Phys. 19, 023054 (2017).

[11] R. Kerviche, S. Guha, and A. Ashok, Fundamental limit of resolving two point sources limited by an arbitrary point spread function, in IEEE International Symposium on Information Theory (ISIT), 2017 (IEEE, New York, 2017), pp. 441–445, https://ieeexplore.ieee.org/document/8006566.

[12] S. Z. Ang, R. Nair, and M. Tsang, Quantum limit for two-dimensional resolution of two incoherent optical point sources, Phys. Rev. A 95, 063847 (2017).

[13] A. Chrostowski, R. Demkowicz-Dobrzański, M. Jarzyna, and K. Banaszek, On super-resolution imaging as a multi-parameter estimation problem, Int. J. Quantum. Inform. 15, 1740005 (2017).

[14] J. Řeháček, Z. Hradil, B. Stoklasa, M. Paúr, J. Grover, A. Krzic, and L. L. Sánchez-Soto, Multiparameter quantum metrology of incoherent point sources: Towards realistic superresolution, Phys. Rev. A 96, 062107 (2017).

[15] J. Řeháček, M. Paúr, B. Stoklasa, Z. Hradil, and L. Sánchez-Soto, Optimal measurements for resolution beyond the rayleigh limit, Opt. Lett. 42, 231 (2017).

[16] J. Řeháček, Z. Hradil, D. Koutný, J. Grover, A. Krzic, and L. L. Sánchez-Soto, Optimal measurements for quantum spatial superresolution, Phys. Rev. A 98, 012103 (2018).

[17] S. Zhou and L. Jiang, Modern description of Rayleigh's criterion, Phys. Rev. A 99, 013808 (2019).

[18] M. Tsang, Quantum limit to subdiffraction incoherent optical imaging, Phys. Rev. A 99, 012305 (2019).

[19] C. W. Helstrom, Quantum Detection and Estimation Theory (Academic Press, New York, 1976).

[20] S. L. Braunstein and C. M. Caves, Statistical Distance and the Geometry of Quantum States, Phys. Rev. Lett. 72, 3439 (1994).

[21] M. G. A. Paris, Quantum estimation for quantum technology, Int. J. Quantum. Inform. 07, 125 (2009).

[22] V. Giovannetti, S. Lloyd, and L. Maccone, Advances in quantum metrology, Nat. Photonics 5, 222 (2011).

[23] F. Yang, A. Tashchilina, E. S. Moiseev, C. Simon, and A. I. Lvovsky, Far-field linear optical superresolution via heterodyne detection in a higher-order local oscillator mode, Optica 3, 1148 (2016).

[24] M. Paúr, B. Stoklasa, Z. Hradil, L. L. Sánchez-Soto, and J. Rehacek, Achieving the ultimate optical resolution, Optica 3, 1144 (2016).

[25] Z. S. Tang, K. Durak, and A. Ling, Fault-tolerant and finite-error localization for point emitters within the diffraction limit, in Frontiers in Optics 2016 (Optical Society of America, Washington, 2016), p. FTu2F.6, https://www.osapublishing.org/abstract.cfm?URI=FiO-2016-FTu2F.6.

[26] W.-K. Tham, H. Ferretti, and A. M. Steinberg, Beating Rayleigh's Curse by Imaging Using Phase Information, Phys. Rev. Lett. 118, 070801 (2017).

[27] R. Leach, C. Evans, L. He, A. Davies, A. Duparr, A. Henning, C. W. Jones, and D. O'Connor, Open questions in surface topography measurement: A roadmap, Surf. Topogr.: Metrol. Prop. 3, 013001 (2015).

[28] X. C. de Lega and P. J. de Groot, Lateral resolution and instrument transfer function as criteria for selecting surface metrology instruments, in Optical Fabrication and Testing (Optical Society of America, Washington, 2012), pp. OTu1D–4, https://www.osapublishing.org/abstract.cfm?uri=OFT-2012-OTu1D.4.

[29] K. Matsumoto, A new approach to the Cramér-Rao-type bound of the pure-state model, J. Phys. A 35, 3111 (2002).

[30] G. Tóth and I. Apellaniz, Quantum metrology from a quantum information science perspective, J. Phys. A 47, 424006 (2014).

[31] M. Szczykulska, T. Baumgratz, and A. Datta, Multi-parameter quantum metrology, Adv. Phys.: X 1, 621 (2016).

[32] S. Ragy, M. Jarzyna, and R. Demkowicz-Dobrzański, Compatibility in multiparameter quantum metrology, Phys. Rev. A 94, 052108 (2016).

[33] D. Braun, G. Adesso, F. Benatti, R. Floreanini, U. Marzolino, M. W. Mitchell, and S. Pirandola, Quantum-enhanced measurements without entanglement, Rev. Mod. Phys. 90, 035006 (2018).

[34] L. Pezzè, A. Smerzi, M. K. Oberthaler, R. Schmied, and P. Treutlein, Quantum metrology with nonclassical states of atomic ensembles, Rev. Mod. Phys. 90, 035005 (2018).

[35] A. Monras and F. Illuminati, Measurement of damping and temperature: Precision bounds in Gaussian dissipative channels, Phys. Rev. A 83, 012315 (2011).

[36] M. G. Genoni, M. G. A. Paris, G. Adesso, H. Nha, P. L. Knight, and M. S. Kim, Optimal estimation of joint parameters in phase space, Phys. Rev. A 87, 012107 (2013).

[37] S. Steinlechner, J. Bauchrowitz, M. Meinders, H. Müller-Ebhardt, K. Danzmann, and R. Schnabel, Quantum-dense metrology, Nat. Photonics 7, 626 (2013).

[38] O. Pinel, P. Jian, N. Treps, C. Fabre, and D. Braun, Quantum parameter estimation using general single-mode Gaussian states, Phys. Rev. A 88, 040102(R) (2013).

[39] P. C. Humphreys, M. Barbieri, A. Datta, and I. A. Walmsley, Quantum Enhanced Multiple Phase Estimation, Phys. Rev. Lett. 111, 070403 (2013).

[40] P. J. D. Crowley, A. Datta, M. Barbieri, and I. A. Walmsley, Tradeoff in simultaneous quantum-limited phase and loss estimation in interferometry, Phys. Rev. A 89, 023845 (2014).

[41] M. D. Vidrighin, G. Donati, M. G. Genoni, X.-M. Jin, W. S. Kolthammer, M. Kim, A. Datta, M. Barbieri, and I. A. Walmsley, Joint estimation of phase and phase diffusion for quantum metrology, Nat. Commun. 5, 3532 (2014).

[42] L. Banchi, S. L. Braunstein, and S. Pirandola, Quantum Fidelity for Arbitrary Gaussian States, Phys. Rev. Lett. 115, 260501 (2015).

[43] T. Baumgratz and A. Datta, Quantum Enhanced Estimation of a Multidimensional Field, Phys. Rev. Lett. **116**, 030801 (2016).

[44] M. Altorio, M. G. Genoni, F. Somma, and M. Barbieri, Metrology with Unknown Detectors, Phys. Rev. Lett. **116**, 100802 (2016).

[45] S. Pirandola and C. Lupo, Ultimate Precision of Adaptive Noise Estimation, Phys. Rev. Lett. **118**, 100502 (2017).

[46] L. Pezzè, M. A. Ciampini, N. Spagnolo, P. C. Humphreys, A. Datta, I. A. Walmsley, M. Barbieri, F. Sciarrino, and A. Smerzi, Optimal Measurements for Simultaneous Quantum Estimation of Multiple Phases, Phys. Rev. Lett. **119**, 130504 (2017).

[47] E. Roccia, I. Gianani, L. Mancino, M. Sbroscia, F. Somma, M. G. Genoni, and M. Barbieri, Entangling measurements for multiparameter estimation with two qubits, Quantum Sci. Technol. **3**, 01LT01 (2018).

[48] R. Yousefjani, R. Nichols, S. Salimi, and G. Adesso, Estimating phase with a random generator: Strategies and resources in multiparameter quantum metrology, Phys. Rev. A **95**, 062307 (2017).

[49] R. Nichols, P. Liuzzo-Scorpo, P. A. Knott, and G. Adesso, Multiparameter gaussian quantum metrology, Phys. Rev. A **98**, 012114 (2018).

[50] T. J. Proctor, P. A. Knott, and J. A. Dunningham, Multi-parameter Estimation in Networked Quantum Sensors, Phys. Rev. Lett. **120**, 080501 (2018).

[51] R. Nair, Quantum-limited loss sensing: Multiparameter Estimation and Bures Distance Between loss channels, Phys. Rev. Lett. **121**, 230801 (2018).

[52] A. Labeyrie, S. G. Lipson, and P. Nisenson, *An Introduction to Optical Stellar Interferometry* (Cambridge University Press, Cambridge, England, 2006).

[53] J. Zmuidzinas, Cramer–Rao sensitivity limits for astronomical instruments: Implications for interferometer design, J. Opt. Soc. Am. A **20**, 218 (2003).

[54] J. W. Goodman, *Statistical Optics* (John Wiley & Sons, New York, 2015).

[55] L. Mandel and E. Wolf, *Optical Coherence and Quantum Optics* (Cambridge University Press, Cambridge, England, 1995).

[56] L. Mandel, Fluctuations of photon beams: The distribution of the photo-electrons, Proc. Phys. Soc. London **74**, 233 (1959).

[57] D. Gottesman, T. Jennewein, and S. Croke, Longer-Baseline Telescopes Using Quantum Repeaters, Phys. Rev. Lett. **109**, 070503 (2012).

[58] M. Tsang, Quantum Nonlocality in Weak-Thermal-Light Interferometry, Phys. Rev. Lett. **107**, 270402 (2011).

[59] However, the assumption of weak sources can be lifted as in Refs. [8,9], leading to similar qualitative results for thermal sources of arbitrary intensity.

[60] M. Tsang, Quantum limits to optical point-source localization, Optica **2**, 646 (2015).

[61] See Supplemental Material at http://link.aps.org/supplemental/10.1103/PhysRevLett.122.140505 for additional technical details.

[62] O. Svelto and D. C. Hanna, *Principles of Lasers* (Springer, New York, 1998).

[63] J. Yang, S. Pang, Y. Zhou, and A. N. Jordan, Optimal measurements for quantum multi-parameter estimation with general states, arXiv:1806.07337.

[64] J. Wolf, Coherent quantum control in biological systems, in *Biophotonics: Spectroscopy, Imaging, Sensing, and Manipulation* (Springer, New York, 2011), pp. 183–201.

[65] Z. Yu and S. Prasad, Quantum Limited Superresolution of an Incoherent Source Pair in Three Dimensions, Phys. Rev. Lett. **121**, 180504 (2018).